A global climate system perspective on African environmental change

Alessandra Giannini
Corresponding author - *International Research Institute for Climate and Society, Earth Institute at Columbia University, 61 Rt 9W, Palisades NY 10964, U.S.A. phone/fax: +1 845 680-4473/4864. email: alesall@iri.columbia.edu*

Michela Biasutti
Lamont-Doherty Earth Observatory, Earth Institute at Columbia University, Palisades NY 10964, U.S.A.

Isaac M. Held
Geophysical Fluid Dynamics Laboratory/NOAA, Princeton NJ 08542, U.S.A.

Adam H. Sobel
Departments of Applied Physics and Applied Math, and Earth and Environmental Sciences, Columbia University, New York NY 10025, U.S.A.

September 5, 2006

Abstract. We review recent advances and current challenges in African climate research and offer a global climate context in which to interpret African environmental change. We classify the various mechanisms that have been proposed as relevant for understanding variations in African rainfall, emphasizing a "tropospheric stabilization" mechanism that is of importance on interannual time scales as well as for the future response to warming oceans.

We show that the latest generation of climate models captures in part the recent African drying trend, attributing it to the combination of anthropogenic emissions of aerosols and greenhouse gases, the relative contribution of which is difficult to quantify with the existing model archive. The same climate models fail to reach a robust agreement regarding the 21^{st} century outlook for African rainfall, in a future with increasing greenhouse gases and decreasing aerosol loadings.

We argue that consideration of African environments in a global climate context is indispensable if we are to exploit advances in our physical understanding of recent variability and trends to shape our outlook on future climate change, to inform the debate between proponents of mitigation v. adaptation strategies, and to plan and implement well-informed policymaking action at national, regional and continental scales

Keywords: Africa, climate and environmental change

1. Introduction

This paper discusses the global-scale mechanisms that affect African rainfall with the goal of placing African environmental change in the context of the global climate change debate, to enable climate science to play an appropriate role in discussions of African development. Motivation comes from recent advances in our physical understanding of African environmental change that point to global climate as a significant agent, while at the same time questioning the effectiveness of local human activity in modifying it.

We focus on the recent observed record of continental-scale tropical African climate variability and on simulations of future change to address the following questions: Are there current trends? Is it wise to linearly extrapolate them into the future? The tropical African focus means that this paper excludes the northern and southern extremities of the continent, whose Mediterranean climates are strongly influenced by extratropical atmospheric circulations. The focus on seasonal-to-interannual and longer-term climate variability derives from our ultimate goal of projecting future African climate change. While a detailed analysis is still premature, we anticipate that projections on regional, rather than continental, scale will become more useful as our outlook on the future becomes less uncertain. Translating a climate outlook on the continental scale—say, for example, a continent-wide drying—into information useful at the regional scale—say, for example, a postponement of the West African monsoon onset, or a change in duration or frequency of dry spells within the southern African wet season—remains a challenge that will only be met by integrating scientific capacity with stakeholders' demand for climate information (Washington et al. 2004; IRI 2006).

In Section 2 we review the climatological seasonal cycle over Africa and introduce relevant governing mechanisms. Section 3 is about climate variability and change during the 20^{th} century, with emphasis on recent decades, as observed, and as simulated in state-of-the-art coupled ocean-atmosphere models. The emphasis is on continental-scale patterns, such as a multi-decadal drying, and the impact of the El Niño-Southern Oscillation (ENSO). Section 4 describes the uncertainties in projections of African climate change and discusses the large-scale mechanisms that we see to be potentially involved. Section 5 offers conclusions and recommendations.

2. Dynamics of tropical rainfall and seasonality of African climate

Deep convection is the physical process which brings about most precipitation in the tropics. It is the result of a hydrodynamic instability in which fluid rises through the depth of the troposphere[1] due to its being lighter than the fluid surrounding it, while heavier fluid sinks, much like water in a pot heated from below. In the atmosphere, the heating from below is due originally to solar radiation, much of which passes through the atmosphere to heat the surface (whether ocean or land). The surface returns that energy to the atmosphere partly by infrared radiation, but also by turbulent fluxes of sensible heat (that which directly influences temperature) and, more quantitatively important in most tropical regions, latent heat in the form of water vapor. The fact that this vapor can be transported for large distances before releasing its latent heat gives tropical climate dynamics much of its distinctive flavor and complexity.

Deep convection can be thought of as a two-step process: first, surface air is warmed or moistened. The warming itself is never large enough to create the low densities needed to convect through the depth of the troposphere. Rather, the water vapor in the air must be sufficient so that when lifted and cooled, by small-scale turbulence or a large-scale weather disturbance, enough condensation will occur, and enough latent heat will be released to render the parcel sufficiently buoyant to ascend through the depth of the troposphere. In the process the parcel will return most of its original water vapor to the surface in the form of precipitation. The key step is the initial warming and moistening of the surface air, a transformation which renders it potentially light enough to ascend through the troposphere. Note also that a warmer (and thus lighter) troposphere above the surface will suppress deep convection since the near-surface air must then become lighter still in order to become buoyant.

Since tropical precipitation is a response to instability, one way to perturb the system is to change its stability, either by changing the temperature and humidity of near-surface air, or by changing the temperature of the atmosphere at higher levels. It is a fundamental feature of the tropical atmosphere that it cannot sustain large horizontal temperature gradients above the planetary boundary layer (that is, more than 1-2 kilometers above the surface). Warming generated by heating of one part of the tropical atmosphere is efficiently distributed horizontally throughout the tropics. A warming of the air above the planetary boundary layer over the Indian Ocean for example, once communicated to Africa

[1] The lowest 15-20 kilometers of the Earth's atmosphere, containing 90% of the atmosphere's mass.

by atmospheric dynamics, would reduce the instability of a boundary layer parcel, and thus inhibit precipitation (Chiang and Sobel 2002). We refer to this mechanism as *stabilization*.

Another way to perturb the system is to change the supply of moisture flowing into the region of interest. Arguments to this effect tend not to directly address the stability properties of the atmospheric column, but instead treat the moisture budget as central. The idea is that other factors, such as gradients in sea surface temperature (Lindzen and Nigam 1987), or the temperature contrast between land and sea (Webster 1994; Hastenrath 1991), induce changes in the pressure field, and thus in the large-scale flow field, so as to alter the low-level convergence of moisture into the region. Since precipitation in rainy regions is largely fed by this moisture convergence rather than by local evaporation, this leads to changes in rainfall. We label this mechanism *moisture supply*.

We will refer to these mechanisms, stabilization and moisture supply, in our discussion of African climate variability and change in the sections to follow.

[Figure 1 here]

Seasons over Africa, as elsewhere, result from interactions between atmosphere, land and ocean as they respond to the annual cycle of insolation—the ultimate driving force behind the alternation of wet and dry, warm and cold seasons. The seasonal climatology of African precipitation is shown in figure 1; heavy rain occurs in a zonally symmetric[2], meridionally confined band, or rainbelt, which straddles the equator near the equinoxes, in April and October, and moves off into the summer hemisphere otherwise, to northern Africa in July and to southern Africa in January. Deep convection and precipitation are spatially confined. In regions of strong precipitation near-surface convergence brings in moisture from surrounding regions, allowing the rainfall to greatly exceed evaporation from the local surface. For this reason, some regions of deep convection are also referred to as Inter-Tropical Convergence Zones, or ITCZs.

Continental surfaces respond immediately to the seasonal cycle of insolation, given the negligible thermal capacity of land, hence land surface temperatures peak right after the passing of the sun overhead, or after the local summer solstice at tropical latitudes. Ocean surfaces respond with a delay, due to the large thermal capacity of the layer of water through which this heat is immediately mixed, hence

[2] Zonal refers to the longitudinal, or east-west direction, while meridional refers to the latitudinal, or north-south direction. Likewise, zonally or meridionally symmetric refers to a feature that characterizes all longitudes or latitudes in a given domain.

they are typically warmest close to the fall equinox. As the rainbelt progresses poleward in its annual migration following the sun, near-surface winds supply moisture to it mostly from its equatorward side. As the rainbelt retreats, dry winds, e.g. the Harmattan winds of the Sahara/Sahel, establish themselves on its poleward side. A large-scale circulation connects near-surface convergence and ascent localized in the rainbelt, to upper-level divergence and generalized descent elsewhere. This meridional migration of the rainbelt produces a single-peaked rainy season at the poleward edges of the tropical region. Due to the additional, non-negligible influence of the ocean, peak rainfall occurs with a delay compared to peak temperature (Biasutti et al. 2003), i.e. sometime between summer solstice and fall equinox—in August in the northern hemisphere, and in February in the southern hemisphere. At latitudes closer to the equator, the rainy season is double-peaked, with a dry season in winter, maxima in spring and fall, and a mid-summer break in between. In figure 1, in comparing the July and January panels, one also notes the seasonal reversal of the prevalent near-surface wind direction typical of monsoon climates, i.e. those climates characterized by a single rainy season and a prolonged dry season.

The role of insolation as a fundamental driver of African climate has been highlighted by paleo-climate studies. The paleo-climatic record unquestionably shows a “green Sahara” in past periods, so much wetter than today that it could sustain a savanna ecosystem in the Tassili-n’Ajjer mountain range of Algeria, located at 25°N, as recently as 6,000 years ago (see Brooks 2004 for a review, and references therein; Petit-Maire 2002). This is explained by an increase in summer insolation due to periodic variations in the Earth’s orbit. Due to the increase in summer insolation, monsoonal rains are driven northwards further into subtropical latitudes. These paleoclimates provide valuable tests of climate models’ sensitivity to changes in insolation. Indeed it has proven difficult to simulate the magnitude of these changes without taking into account feedbacks in the oceans and in terrestrial vegetation (e.g. Braconnot et al. 1999).

The potential for changes in insolation to alter African climate also inspired early attempts to explain African rainfall variability in terms of “desertification” (e.g. Charney 1975). A key element in this picture is that human activity reduces vegetation cover, which increases the albedo (i.e. reflectivity) of the surface, resulting in less absorbed solar radiation. In analogy with theories of the “Green Sahara”, this reduction in absorbed energy in turn results in a reduction in precipitation. This paradigm for African climate change emerged shortly after inception of the Sahel drought, in the early 1970s, and

has remained in the popular imagination since. In the climate science community the desertification paradigm has in fact been supplanted by an alternative that is in many respects its exact opposite—that African rainfall variability is primarily driven by changes in remote sea surface temperatures, rather than in local properties of the land surface itself. Before addressing this issue directly we review some aspects of the observations of African climate variability through the 20^{th} century.

3. African climate of the 20th century

In this section we first describe temporal (section 3.1) and spatio-temporal (section 3.2) patterns of observed African rainfall variability, relating them to the relevant literature on regional climate. We then compare such patterns with those simulated by a large number of coupled ocean-atmosphere models forced by the 20th century trajectory of anthropogenic aerosol and greenhouse gas emissions (section 3.3).

We base our observational analyses[3] on the gridded precipitation dataset produced by the Climatic Research Unit of the University of East Anglia (CRU; Hulme 1992). Our baseline analyses cover the period 1930-1995, though in Section 3.1 we extend temporal coverage to the present, using Global Precipitation Climatology Project (GPCP; Huffman et al. 1997) data, a blended satellite-rain gauge product with global, i.e. land and ocean, coverage, available starting in 1979. The period from the 1930s to the mid-1990s affords an appropriate observational coverage over Africa. Coverage as measured by the number of stations recording monthly in the archives of the Global Historical Climate Network (GHCN; Vose et al. 1992), stored at the U.S. National Oceanic and Atmospheric Administration's National Climate Data Center, is best in mid-century, and declines towards the beginning and end (not shown).

[3] All observational datasets mentioned in this paragraph—CRU, GHCN and GPCP by their acronyms—are available via the International Research Institute for Climate and Society (IRI)'s Data Library *http://iridl.ldeo.columbia.edu/index.html*.

3.1. Regional variability in time (1930-2005)

Based on considerations of seasonality—which distinguishes monsoonal from equatorial climates (see previous section)—and of regional political entities, we define three sub-regions; western (0°to 20°N, 20°W to 20°E), eastern equatorial (10°S to 10°N, 20°E to 50°E), and southern Africa (25°S to 10°S, 20°E to 40°E). The history of annual-mean (July to June) rainfall anomalies averaged over these regions is displayed in figure 2.

[Figure 2 here]

Comparison of the three panels in figure 2 highlights the qualitative difference between the West African time series on one side, and its eastern equatorial and southern African counterparts on the other. The former is characterized by a high degree of persistence, of anomalously wet (e.g. in the 1930s, 1950s and 1960s) and dry (e.g. in the 1970s and 1980s) years, while in the latter interannual variability is greater. As will become apparent in the next subsection, this has to do with the time scales favored by the oceanic forcings effecting these changes. Also noticeable is how in recent decades, as West Africa has witnessed a partial recovery of the rains (e.g. Nicholson (2005) in the case of the Sahel), eastern equatorial and southern Africa seem to have suffered from more frequent anomalously dry events. The trend towards dry conditions is made even more apparent with the GPCP extension of the time series—the continuous red line in figure 2—particularly for eastern equatorial Africa.

3.2. Spatio-temporal patterns of African climate variability

To identify patterns of African climate variability at the continental scale, and to connect these patterns to common, global-scale forcings, we use Principal Component Analysis (PCA; von Storch and Zwiers 1999), a statistical technique widely used in the Earth and social sciences, and linear regression. In our analysis, PCA objectively identifies spatial patterns that express co-variability in time across all tropical African grid points in the CRU dataset. By maximizing the variance captured in the first such pattern, and in subsequent orthogonal, or independent, patterns, PCA identifies broad spatial features, allowing one to summarize a large fraction of the information with a small number of time series. We apply PCA to annual-mean (July-June) precipitation anomalies, with respect to the long-term mean, in the domain

between 35°S and 30°N, 20°W and 60°E[4]. We apply linear regression to relate the temporal variability associated with the spatial patterns identified by PCA to other aspects of the global ocean-atmosphere system.

[Figure 3 here]

Statistical analysis of African rainfall variability has a long history. In one of the first continental-scale studies Nicholson (1986) identified two recurrent spatial patterns over Africa. One was characterized by continent-wide anomalies of the same sign, the other by anomalies of opposite sign at equatorial latitudes and at the poleward margins of monsoon regions. Nicholson's findings are echoed in our analysis (figure 3). Three patterns stand out; one exemplifies a continent-wide drying most significant at the poleward edges of the monsoons, and the other two the influence of ENSO[5], dominant on eastern equatorial and southern Africa. The three patterns combined capture 37% of the total variance in precipitation over the tropical African domain considered. Our discussion in the following subsections will focus on these patterns. That they are actually representative of regional anomalies is demonstrated by the significant correlation of their associated time series (figures 3d,e,f) with the regional averages described in the previous subsection (over 1930-1995); the West African average is unequivocally correlated with the "continental drying" pattern (correlation is 0.97), while eastern equatorial and southern African averages are correlated with both "drying" and "ENSO" patterns (with correlations of the order of 0.5).

3.2.1. *A continental precipitation pattern and its relation to global ocean temperature*

The leading pattern of annual-mean variability in precipitation over 1930-1995 is displayed in figure 3, left column. The spatial pattern (figure 3a) is continental in scale. It takes on stronger values in the northern hemisphere, including in the Sahel and along coastal Gulf of Guinea, and weaker, but significant values at tropical latitudes over southern Africa. In fact, this pattern resembles that of the linear trend computed over the same period (not shown)—an overall drying trend. However, the linear

[4] This analysis was repeated on GHCN station data on a shorter period (1950-1995; not shown), yielding consistent results.

[5] A coupled ocean-atmosphere phenomenon which originates in the tropical Pacific, and has world-wide impacts (see Wallace et al. 1998, and accompanying articles in the same issue of *J. Geophys. Res.*). ENSO-related variability can be identified by its preferred interannual time scale, given that an ENSO event usually recurs every 2 to 7 years.

trend does not capture all the important features of the time series associated with the pattern shown in figure 3. Fluctuations with a multidecadal time scale superimposed on year-to-year variations are evident in figure 3d: the 1950s and 1960s were clearly wetter than the long-term average, but so were the 1930s. The wetter-than-average central decades of the 20th century certainly contribute to making the contrast with the drier decades that followed, in the 1970s and 1980s, even starker. This pattern is statistically related to global SSTs, with the sign such that drying over Africa is associated with warmer tropical Pacific, Indian and South Atlantic Oceans, and a cooler North Atlantic basin (figure 3g; Folland et al. 1986; Giannini et al. 2003).

In the northern hemisphere this drying pattern combines features expressed seasonally in spring and summer respectively along coastal Gulf of Guinea and across the Sahel (not shown; Wagner and DaSilva 1994; Nicholson 1981; Lamb and Peppler 1992; Janicot et al. 1996). Previous studies have proposed two explanations for the influence of oceanic temperatures on West African rainfall. The first one is a *moisture supply* argument, articulated by Lamb (1978) and Folland et al. (1986), and more recently by Rotstayn and Lohmann (2002) and Hoerling et al. (2006). It emphasizes the role of the north/south SST gradient, which is particularly evident in the Atlantic basin (figure 3g). This explanation relates the recent, persistent drying of the Sahel to an equatorward shift of the mean location of the Atlantic ITCZ, connecting reduced oceanic precipitation with a weaker West African monsoonal flow. A complementary explanation, consistent with the modeling results of Giannini et al. (2003), Bader and Latif (2003) and Lu and Delworth (2005), and with the idealized study of Chiang and Sobel (2002), is a *stabilization* argument in which warmer Indo-Pacific SSTs cause a warming of the entire tropical troposphere, stabilizing the tropical troposphere from above in the Atlantic sector and over Africa. The key to this mechanism is that the continental boundary layer is unable to increase its energy content and buoyancy to keep up with the energy content over the surrounding oceans. The issue of whether West African rainfall is affected not only by ocean temperature gradients, but also by spatially uniform increases in oceanic temperatures, is central to projections of climate change in the 21^{st} century.

In the southern hemisphere the indication for a recent, persistent drying is significant, but not as strong as in the northern hemisphere. When southern Africa is considered in isolation, a significant drying trend is seen since the 1970s (Nicholson 1993; Mason and Tyson 2000), but not on longer, centennial timescales (Fauchereau et al. 2003). As we will show in the next subsection, ENSO is the

dominant influence on the predictable component of interannual rainfall variability in eastern equatorial and southern Africa. Nevertheless, anthropogenic influences cannot be ruled out. To find out more about the combined effects of ENSO and climate change on southern Africa the reader is referred to Mason (2001). One possibility is that the drying signal in southeastern Africa is due in part to the warming trend in the Indian Ocean (Hoerling et al. 2006), which is understood to enhance the drying impact of warm ENSO events on this region (Richard et al. 2000). Another possibility is that global warming has caused the recent trend towards more frequent and persistent warm ENSO events (Timmermann et al. 1999, Trenberth and Hoar 1997), thus affecting Southern African rainfall indirectly. Whether this is the case is still matter of debate (Houghton et al. 2001).

3.2.2. *Interannual variability related to ENSO*

ENSO is the dominant phenomenon in the two remaining patterns (figure 3, center and right columns). Its signature in SST—anomalies of one sign centered on the equator in the central and eastern tropical Pacific basin surrounded by anomalies of the opposite sign at subtropical latitudes, in the characteristic "horseshoe" pattern (Rasmusson and Carpenter 1982)—is clear in figures 3h,i. ENSO has a large impact on rainfall in eastern equatorial and southern Africa (Ropelewski and Halpert 1987; Ogallo 1989; Nicholson and Kim 1997; Goddard and Graham 1999; Schreck and Semazzi 2004; Cane et al. 1994; Unganai 1996; Mason 2001; Mulenga et al. 2003; Reason and Jagadheesha 2005), as depicted in figures 3b,c. However, it is also understood to have a non-negligible effect north of the equator (Seleshi and Demaree 1995; Janicot et al. 1996; Ward 1998; Rowell 2001; Giannini et al. 2003), especially when care is taken to separate the year-to-year from the multi-decadal variability described in the previous subsection.

ENSO impacts Africa directly via an atmospheric teleconnection (Glantz et al. 1991; Wallace et al. 1998) and indirectly, via the response of the Indian and Atlantic basins to it (Klein et al. 1999; Alexander et al. 2002). The direct influence of ENSO over Africa follows the path outlined above for the influence of the Indo-Pacific warming trend under the *stabilization* mechanism. The entire tropical troposphere warms during a warm ENSO, or El Niño event[6] as a response to the warming of central and

[6] To the extent that the system is linear, all features described for a warm ENSO, or El Ni˜no event, are reversed in sign for a cold ENSO, or La Ni˜na event.

eastern equatorial Pacific (Yulaeva and Wallace 1994, Soden 2000, Sobel et al. 2002). Outside the central and eastern equatorial Pacific, stabilization of the atmospheric column initially leads to below-average precipitation in remote regions (Chiang and Sobel 2002), as is observed during the growth phase of warm ENSO events, which coincides with the northern hemisphere monsoon season in South and East Asia, Africa and Central America (Ropelewski and Halpert 1987; Kiladis and Diaz 1989; Lyon 2004).

The third pattern captures this pure atmospheric influence—note how the tropical Pacific SST anomalies in figure 3i dwarf any signal in the ocean basins around Africa. The atmospheric signal is indeed a drying in the case of a warm ENSO event, as discussed by Goddard and Graham (1999) in the context of comprehensive climate model simulations, and explained by Chiang and Sobel (2002) in an idealized framework. In our analysis this signal is strongest in eastern Africa between the equator and 20°S.

The second pattern represents the "canonical" ENSO influence, one that combines the effects of remote, or tropical Pacific, and local, especially Indian Ocean, surface temperatures (figure 3h). It captures the wetter than average conditions over eastern equatorial Africa known to be a maximum during the October-December short rains, which coincide with mature warm ENSO conditions, as well as the drier than average conditions over southern Africa known to be most prominent in the January-March season immediately subsequent to the mature phase (figure 3b). The Indian Ocean SST anomalies associated with the dipolar rainfall pattern between eastern equatorial and southern Africa are related in part to ENSO. Due to their thermal inertia, the remote tropical oceans warm in response to the ENSO-induced changes in the tropospheric temperature with a lag of a few months (see, e.g. Klein et al. 1999; Chiang and Sobel 2002; Sobel et al. 2002; Chiang and Lintner 2005). In some remote oceanic regions, ENSO-induced changes in surface wind stress can induce an additional SST increase via ocean dynamics (e.g. Bracco et al. 2005; Song et al. 2006 in the case of the Indian Ocean), hence reversing the initial direct atmospheric stabilization and leading to destabilization of the tropical troposphere from the bottom up. This effect, together with an increased moisture transport associated with enhanced evaporation over the warmer than average Indian Ocean, can lead to positive precipitation anomalies for eastern equatorial Africa (Goddard and Graham 1999). Hence in this region a warm ENSO can induce below-average precipitation when the atmospheric bridge dominates, as depicted in the third pattern, or it can result in above-average precipitation, when the dynamically-induced Indian Ocean response overwhelms the remote atmospheric effect, as in the second pattern. Song et al. (2006) have recently argued that the

timing of ENSO with respect to the seasonal cycle of upwelling in the eastern Indian Ocean helps determine whether the dynamic Indian Ocean component visible in figure 3b becomes dominant.

To summarize, when observations of precipitation over Africa are analyzed with a view to their global linkages, two continental-scale patterns, related to variability in the oceans, appear to dominate African climate variability: (1) a continental-scale drying pattern related to enhanced warming of the southern compared to the northern tropics and to a warming of the tropical oceans, (2) the impact of ENSO on the tropical atmosphere and oceans around Africa.

3.3. LATE 20TH CENTURY CLIMATE CHANGE IN RECENT SIMULATIONS

In early 2005, simulations with state-of-the-art climate models from 16 research centers were made available to the scientific community by the Intergovernmental Panel on Climate Change (IPCC) through the Program for Climate Modeling Diagnosis and Intercomparison (PCMDI; *http://www-pcmdi.llnl.gov/ipcc/about_ipcc.php*) in preparation for the IPCC's 4th assessment report (4AR) to be published in 2007. In this subsection and the next section we discuss our analysis of 20th and 21st century simulations of African climate change with 19 different models taken from the IPCC/PCMDI archive (Biasutti and Giannini 2006). Lau et al. (2006) and Cook and Vizy (2006) provide other valuable analyses of the same archive of simulations.

In this subsection we discuss the comparison between simulations obtained with the same climate models integrated under two different protocols. In one case—the control, or pre-industrial (PI) simulations—aerosol and greenhouse gas emissions are set to constant values representative of conditions before anthropogenic contributions to these climate forcings became significant. In the other—the forced, or 20th century (XX) simulations—the historical progression of emissions associated with industrialization, which constitute the anthropogenic forcing[7], is introduced, and influences the evolution of the climate system from the second half of the 19th century to the present.

[7] Certain models also include natural variability associated with changes in insolation, and volcanic aerosols, as well as land use/land cover change, in their 20th century simulations.

While the historical concentrations of anthropogenic greenhouse gases are fairly accurately inferred from fossil fuel extraction records, the historical concentration, type, and spatial distribution of aerosols remain uncertain (IPCC 2001). The response of the climate system can vary greatly depending on whether the forcing includes only predominantly reflecting aerosols, e.g. sulfate aerosols, or both reflecting and absorbing aerosols, e.g. black carbon, (e.g. Menon et al. 2002). Furthermore, only a few models include parameterizations of the indirect effects of aerosols, i.e. those occurring via the aerosols' interaction with cloud microphysics and precipitation efficiency (Lohmann et al. 2000). However, as disparate as the diagnosis or prognosis of the aerosols' impact may be, when the forced, or 20th century (XX) simulations, are compared to the control, or pre-industrial (PI) simulations, features that are consistent across models can be identified in the surface temperature and precipitation fields.

Multi-model ensemble averages of annual-mean surface temperature and precipitation are presented in the subsections that follow. Multi-model ensemble averaging (see e.g. Krishnamurti et al. 1999; Barnston et al. 2003; Hagedorn et al. 2005 in the context of seasonal climate prediction) is one way to deal with uncertainties related to parameterizations, i.e. those components of the models that represent processes that cannot be simulated from first principles, whether because of finite computational resources or incomplete knowledge of the governing physics. The hope is that differences among models that are not physical will cancel, while common robust responses will be retained. Figure 4 shows the changes in annual-mean surface temperature and precipitation between the last 25 years of the 20th century (XX) and a 25-year period in the pre-industrial (PI) simulations, i.e. the XX-PI difference (Biasutti and Giannini 2006). The top panels show the average of all models, the bottom panels a measure of inter-model agreement (see caption for details).

[Figure 4 here]

3.3.1. *XX-PI changes in surface temperature*

Compared to pre-industrial times, late 20^{th}century annual-mean surface temperature increases less in the mid-latitude extratropics than in the deep tropics and in high latitudes (figure 4a), with many models cooling the mid-latitude northern hemisphere oceans. This modeled response is very similar to the linear trend pattern in observed surface temperature computed over 1950-2000 (Hansen et al. 1999; *http://data.giss.nasa.gov/gistemp/maps/*), in both spatial signature and amplitude. This pattern has been

the subject of intensive investigation (see, in past IPCC reports, Santer et. al. 1996 and Mitchell et al. 2001, and, more recently, Stott et al. 2006) and we do not discuss it further here except to note that reflecting sulfate aerosols contribute to minimizing the warming in the northern hemisphere in the model simulations.

3.3.2. *XX-PI changes in precipitation*

The XX - PI difference in SST discussed above bears a striking resemblance to that identified by Folland et al. (1986) and Giannini et al. (2003) to have been associated with drought in the Sahel (also see figure 3g here). Consistently, the response pattern in the annual mean (and, more prominently, in the June-August average) of precipitation shows a decrease across the tropical Atlantic ITCZ and into the Sahel in the late 20th century compared to the pre-industrial control. This is echoed in all models, except two which show negligible anomalies (also see figure 2 in Biasutti and Giannini 2006). We conclude that anthropogenic forcings played a non negligible role in the late 20th century drying of the Sahel (Held et al.2005; Biasutti and Giannini 2006; Rotstayn and Lohmann 2002), although there is little doubt that a large fraction of the observed variations in Sahel rainfall was generated by natural SST variability. A rough estimate suggests that the anthropogenic contribution is about 30% of the recent long-term drying trend. The current model archive is not suited to separating the effects of aerosols from those of increasing greenhouse gases. The fact that this 20^{th} century drying trend in the Sahel does not continue into the 21^{st} century in the majority of models (see below) nonetheless strongly suggests that models may be more consistently representing a change in the moisture supply mechanism, in this case expressed in the North-South gradient in SST forced by aerosols, and attendant displacement of the Atlantic ITCZ, rather than in the stabilization mechanism associated with the more uniform tropical SST warming forced by greenhouse gases (Biasutti and Giannini 2006). In one model, that developed at NOAA's Geophysical Fluid Dynamics Laboratory, Held et al. (2005) find a clear signature of drying due to greenhouse gases.

The drying of the Sahel is accompanied, in the annual mean picture, by anomalies in eastern equatorial and southern Africa reminiscent of the response to ENSO, i.e. wet anomalies in eastern equatorial and dry anomalies in southern Africa, but these anomalies are weak and inconsistent across models, even more so during the December-February season (not shown), when the ENSO-related signal should

be most prominent. This lack of agreement would seem surprising, given that models forced with the historic global SST consistently show a drying trend in southern Africa (Hoerling et al. 2006). It is possible that the observed drying trend was a consequence of the prevalence of warm ENSO events at the end of the 20^{th}century, and that coupled models do not simulate such prevalence, either because it is not a forced behavior or because the models' simulation of ENSO is not sufficiently accurate.

4. The uncertain future: a global warming scenario simulation

Climate science has made impressive inroads in understanding climate variability and change. A future, further warming of the planet is predicted with certainty. Yet, the regional patterns of climate change, especially potential future shifts in the spatial distribution of tropical rainfall, remain uncertain. In figure 5 we compare the climate of the late 20th century to that of the late 21st century as simulated in the so-called A1B climate change scenario by the same 19 models introduced in the previous section. In this scenario a growing world economy and the adoption of cleaner technologies combine to give growing greenhouse gas concentrations and declining sulfate aerosol loadings.

[Figure 5 here]

The global warming signature emerges clearly in the annual-mean temperature difference (figure 5a). The models show (i) a more equatorially symmetric warming of the tropical oceans, (ii) a more consistent ENSO signal in the 21^{st}compared to the 20^{th}century, with a pronounced, El Niño-like warming of the central and eastern equatorial Pacific[8], and (iii) a more pronounced land-sea temperature contrast, with warming of the continents that surpasses the warming of the tropical oceans. In Africa, the surface warming is largest in desert regions, and relatively more modest in equatorial regions, where the increased radiative forcing is partly used to evaporate soil moisture.

The precipitation signal is less clear. Over Africa, the multi-model mean in precipitation (figure 5b) suggests more intense rainfall in equatorial regions and drier conditions elsewhere, but this prediction is not unanimous across models (figure 5d): it is more robust in eastern equatorial Africa, where a majority of models agree on a trend towards wetter conditions, but less certain in southern Africa, where there is

[8] but see Collins et al. (2003), on the trustworthiness of an El Ni˜no-like response to global warming.

some indication of a drying trend (Hoerling et al. 2006), but much scatter in the model solutions. There is no agreement on whether the Sahel will be drier or wetter in the future (Held et al. 2005; Biasutti and Giannini 2006; Hoerling et al. 2006; Cook and Vizy 2006). Averages for the same three regions defined in Section 3.1—western, eastern equatorial and southern Africa—in the last 50 years of the 20th century simulations and in the 21st century simulations are plotted in figure 6, for each model, and for the multi-model mean. The scatter among models is the most visible feature.

[Figure 6 here]

These results are based on a uniform weighting of all models in the IPCC/PCMDI archive. But some of the models clearly have better simulations of African rainfall than others (Cook and Vizy 2006). The question of how best to weigh the different projections in such an ensemble of models remains open. There are many possible metrics, some focusing on regional climate simulations and others evaluating the models more globally, some on the behavior of the atmospheric model when run over observed SSTs, and others on the behavior of the coupled system. What is lacking at present is an accepted strategy for determining which metrics are most relevant to evaluate a model's projection of African rainfall.

Partly based on inspection of this model archive we can generate hypotheses that may help clarify why models differ in their 21^{st} century responses. A uniform warming is confidently expected to lead to an increase in specific humidity (Allen and Ingram 2002; Held and Soden 2006). The hypothesis that regional precipitation changes are determined by this humidity change, rather than by changes to the circulation, leads to a prediction of an increase in rainfall in currently rain-rich regions, and a decrease in currently semi-arid regions, a prediction that is borne out in climate simulations in a zonally averaged sense, but not throughout Africa (although it may help in interpreting the projected increase in rainfall in parts of eastern equatorial Africa). A related response, in which the rainiest regions become rainier, and drying occurs at the margins of those regions, is predicted by a climate model of intermediate complexity, in association with circulation as well as humidity changes (Neelin et al. 2003). (iii) El-Niño-like climate change could lead to teleconnections similar to those seen at interannual time scales, which would tend to dry much of the African continent. (iv) An enhanced land-sea temperature contrast, whereby oceans warm less than continents due to land surface or cloud feedbacks, could lead to an intensification of monsoonal circulations, hence an increase in moisture supply and thus rainfall in the Sahel (Haarsma et al. 2005). The current challenge is to determine the relative importance of these

various mechanisms over Africa, and to design metrics that tell us whether the model simulations are adequate to provide a meaningful prediction of future change in African rainfall.

5. Conclusions: the climate of African environmental change

African environmental change has most often been handled as a regional phenomenon with local anthropogenic causes and potentially global effects. The local causes have generally been ascribed to the mismanagement of limited natural resources under the ever-increasing pressure of a growing, vulnerable population—a perverse feedback loop in which the poorest of the poor deprive themselves by impoverishing the environment they depend on for their livelihoods. The global threat posed by African environmental change has often been exaggerated; the relevance of feedbacks between human-induced perturbations of land surface properties, e.g. via changes in land use/land cover, and the global atmospheric circulation, has not been conclusively proven (see Nicholson 2000, and references therein for a review), especially vis à vis the magnitude of the imprint of large-scale patterns of climate variability and change on regional scales.

In contrast, recent advances in the physical understanding of African environmental change point to global climate as a significant agent. These advances include: (i) satellite-based observations of vegetation cover; (ii) modeling of land cover response to land use and to precipitation, and (iii) climate modeling of the response of African rainfall to the observed distribution of sea surface temperatures (SSTs). Satellite-based observations became available in the 1980s, and exposed the ability of vegetation to recover from drought at both seasonal and interannual time-scales once rains return to normal (Tucker et al. 1991; Anyamba and Eastman 1996; Prince et al. 1998; Nicholson et al. 1998; Eklundh and Olsson 2003; Herrmann et al. 2005). Modeling of land cover and climatic responses to land use have begun to converge to relatively modest magnitudes over Africa, and have not indicated an ability to explain the dominant modes of rainfall variability (Taylor et al. 2002; Hickler et al. 2005). Climate models forced only by the observed, long-term history of sea surface temperature have, in sharp contrast, reproduced the historical record of Sahel rainfall (Giannini et al. 2003; Lu and Delworth 2005), confirming the role of the global oceans in pacing drought in the Sahel (Folland et al. 1986; Palmer 1986; Rowell et

al. 1995), as well as, more generally, helping to explain climate variability over Africa (Hoerling et al. 2006).

With this paper we have attempted to widen the perspective on African environmental change by showing how global climate can drive it through large-scale changes in rainfall patterns (also see Hulme et al. 2001). We identified two mechanisms relevant to the recent past and future changes in African rainfall—a moisture supply mechanism, and a stabilization mechanism— and indicated that the competition between the two in a warming world may explain the uncertainties in projections of African rainfall into the next century. Our analysis of annual-mean, continental-scale variability of African precipitation, as observed over the better part of the 20^{th}century and modeled in the IPCC 4AR simulations, supports the link between a trend towards drier conditions for the monsoon regions of Africa over the second half of the 20^{th}century and a pattern of tropical ocean warming (see Sections 3.1 and 3.2). It also highlights the skill of the models currently being analyzed in preparation for IPCC 4AR in reproducing certain large-scale features of 20^{th}century climate (see Section 3.3). In this context, we discussed evidence in support of partial attribution of the recent recurrence of drought in the Sahel to anthropogenic forcings, specifically to the combined effects of aerosols and greenhouse gases (Held et al. 2005, Biasutti and Giannini 2006; Rotstayn and Lohmann 2002). Similarly, we related a drying trend in tropical southern Africa to the warming of the Indian Ocean, while agreeing that its potential anthropogenic origin may have been confounded by the more frequent occurrence of warm ENSO events since the mid-1970s compared to the mid-20th century.

In conclusion, there has been a shift in focus with regard to the causes of changes in African rainfall - from regional land use and land cover changes and the actions of African peoples, to the global distribution of oceanic temperatures, both naturally varying and as influenced by anthropogenic emissions from the industrial north. It is hoped that the global community's "mainstreaming of climate in development", i.e. the inclusion of a global climate change perspective in discussions of African development, will result in renewed consideration of issues of environmental justice and the morality of mitigation vs. adaptation strategies.

Acknowledgements

Jeffrey Sachs, David Battisti, Polly Ericksen, Tsegay Wolde-Georgis, Jian Lu and Tom Delworth for their encouragement, and for sharing their knowledge. Naomi Naik for her technical support, especially for her patience in downloading model output. The Intergovermental Panel on Climate Change (IPCC) and the Program for Climate Modeling Diagnosis and Intercomparison (PCMDI) for making the model output available in preparation of the IPCC's 4th Assessment Report. The Earth Institute at Columbia University's Cross-Cutting Initiative on Climate and Society (led by Mark Cane, Cynthia Rosenzweig and Steve Zebiak), NOAA (AG: Office of Global Programs grant NA07GP0213, MB: grant NAO30AR4320179), and the David and Lucile Packard Foundation Fellowship (MB, AHS) for their financial support.

References

Alexander, M. A., Bladé, I., Newman, M., Lanzante, J. R., Lau, N.-C. and Scott, J. D. 2002: The atmospheric bridge: the influence of ENSO teleconnections on air-sea interaction over the global oceans. *J. Climate*, **15**, 2205–2231.

Allen, M. and Ingram, W. 2002: Constraints on future changes in climate and the hydrological cycle. *Nature*, **419**, 224–232.

Anyamba, A. and Eastman, J. 1996: Interannual variability of NDVI over Africa and its relation to El Ni˜no/Southern Oscillation. *Int. J. Remote Sensing*, **17**, 2533–2548.

Bader, J. and Latif, M. 2003: The impact of decadal-scale Indian Ocean sea surface temperature anomalies on Sahelian rainfall and the North Atlantic Oscillation. *Geophys. Res. Lett.* doi:10.1029/2003GL018426.

Barnston, A. G., Mason, S. J., Goddard, L., DeWitt, D. G. and Zebiak, S. E. 2003: Multimodel ensembling in seasonal climate forecasting at IRI. *Bull. Amer. Meteor. Soc.*, **84**, 1783–1796.

Biasutti, M. and Giannini, A. 2006: Robust Sahel drying in response to late 20th century forcings. *Geophys. Res. Lett.* submitted.

Biasutti, M., Battisti, D. S. and Sarachik, E. S. 2003: The annual cycle over the tropical Atlantic, South America, and Africa. *J. Climate*, **16**, 2491–2508.

Bracco, A., Kucharski, F., Molteni, F., Hazeleger, W. and Severijns, C. 2005: Internal and forced modes of variability in the Indian Ocean. *Geophys. Res. Lett.*, **32**, L12707. doi:10.1029/2005GL023154.

Braconnot, P., Joussaume, S., Marti, O. and deNoblet, N. 1999: Synergistic feedbacks from the ocean and vegetation on the African monsoon response to mid-Holocene insolation. *Geophys. Res. Lett.*, **26(16)**, 2481–2484.

Brooks, N. 2004: Drought in the African Sahel: long term perspectives and future prospects. Tyndall Centre for Climate Change Research, Working paper 61.

Cane, M. A., Eshel, G. and Buckland, R. W. 1994: Forecasting Zimbabwean maize yield using eastern equatorial Pacific sea surface temperature. *Nature*, **370**, 204–205.

Charney, J. 1975: Dynamics of deserts and drought in the Sahel. *Q. J. Roy. Meteor. Soc.*, **101**, 193–202.

Chiang, J. and Lintner, B. 2005: Mechanisms of remote tropical surface warming during El Ni˜no. *J. Climate*, **18**, 4130–4149.

Chiang, J. C. H. and Sobel, A. H. 2002: Tropical tropospheric temperature variations caused by ENSO and their influence on the remote tropical climate. *J. Climate*, **15**, 2616–2631.

Collins, M. and the CMIP Modelling Groups 2003: El Ni˜no or La Ni˜na-like climate change?. *Clim. Dyn.*, **24**, 89–104. doi: 10.1007/s00382-004-0478-x.

Cook, K. H. and Vizy, E. K. 2006: Coupled model simulations of the West African monsoon system: 20th century simulations and 21st century predictions.. *J. Climate*, **19**, 3681–3703.

Eklundh, L. and Olsson, L. 2003: Vegetation index trends for the African Sahel 1982-1999. *Geophys. Res. Lett.* Apr 2003.

Fauchereau, N., Trzaska, S., Rouault, M. and Richard, Y. 2003: Rainfall Variability and Changes in Southern Africa during the 20th Century in the Global Warming Context. *Natural Hazards*, **29**, 139–154. DOI 10.1023/A:1023630924100.

Folland, C. K., Palmer, T. N. and Parker, D. E. 1986: Sahel rainfall and worldwide sea temperatures, 1901-85. *Nature*, **320**, 602–607.

Giannini, A., Saravanan, R. and Chang, P. 2003: Oceanic forcing of Sahel rainfall on interannual to interdecadal time scales. *Science*, **302**, 1027–1030. Published online 9 October 2003. 10.1126/science.1089357.

Glantz, M. H., Katz, R. W. and Nicholls, N. 1991: Teleconnections linking worldwide climate anomalies. Cambridge University Press, 535 pp.

Goddard, L. and Graham, N. E. 1999: Importance of the Indian Ocean for simulating rainfall anomalies over eastern and southern Africa. *J. Geophys. Res.*, **104**, 19099–19116.

Haarsma, R. J., Selten, F., Weber, N. and Kliphuis, M. 2005: Sahel rainfall variability and response to greenhouse warming. *Geophys. Res. Lett.* doi:10.1029/2005GL023232.

Hagedorn, R., Doblas-Reyes, F. and Palmer, T. 2005: The rationale behind the success of multi-model ensembles in seasonal forecasting - I. Basic concept. *Tellus A*, **57**, 219–233. doi:10.1111/j.1600-0870.2005.00103.x.

Hansen, J., Ruedy, R., Glascoe, J. and Sato, M. 1999: GISS analysis of surface temperature change. *J. Geophys. Res. - Atmos.*, **104**, 30997–31022. doi:10.1029/1999JD900835.

Hastenrath, S. 1991: Climate dynamics of the tropics. Kluwer Academic Publishers, Dordrecht, The Netherlands.

Held, I. and Soden, B. 2006: Robust responses of the hydrological cycle to global warming. *J. Climate*. in press.

Herrmann, S. M., Anyamba, A. and Tucker, C. J. 2005: Recent trends in vegetation dynamics in the (A)frican (S)ahel and their relationship to climate. *Global Environ. Change*, **15**, 394–404.

Hickler, T., Eklundh, L., Seaquist, J. W., Smith, B., Ardö, J., Olsson, L., Sykes, M. and Sjöström, M. 2005: Precipitation controls Sahel greening trend. *Geophys. Res. Lett.* doi:10.1029/2005GL024370, L21415.

Hoerling, M. P., Hurrell, J. W., Eischeid, J. and Phillips, A. S. 2006: Detection and attribution of 20th century northern and southern African monsoon change. *J. Climate*, **19**, 3989–4008.

Houghton, J. T., Ding, Y., Griggs, D. J., Noguer, M., van der Linden, P. J., Dai, X., Maskell, K. and Johnson, C. A. 2001: Climate change 2001: the scientific basis. 881 pp. Cambridge University Press.

Huffman, G. J., Adler, R. F., Arkin, P., Chang, A., Ferraro, R., Gruber, A., Janowiak, J., McNab, A., Rudolf, B. and Schneider, U. 1997: The global precipitation climatology project (GPCP) combined precipitation dataset. *Bull. Amer. Meteor. Soc.*, **78**, 5–20.

Hulme, M. 1992: A 1951-80 global land precipitation climatology for the evaluation of general circulation models. *Climate Dyn.*, **7**, 57–72.

Hulme, M., Doherty, R., Ngara, T., New, M. and Lister, D. 2001: African climate change: 1900-2100. *Clim. Res.*, **17**, 145–168.

IRI 2006: A gap analysis for the implementation of the Global Climate Observing System programme in Africa. The International Research Institute for Climate and Society (IRI), in collaboration with Global Climate Observing System (GCOS), United Kingdom's Department for International Development (DfID), and UN Economic Commission for Africa (ECA).

Janicot, S., Moron, V. and Fontaine, B. 1996: Sahel droughts and ENSO dynamics. *Geophys. Res. Lett.*, **23**, 515–518.

Kalnay, E. and Coauthors 1996: The NCEP-NCAR 40-year reanalysis project. *Bull. Amer. Meteor. Soc.*, **77**, 437–471.

Kaplan, A., Cane, M. A., Kushnir, Y., Clement, A. C., Blumenthal, M. B. and Rajagopalan, B. 1998: Analyses of global sea surface temperature 1856-1991. *J. Geophys. Res.*, **103**, 18,567–18,589.

Kiladis, G. N. and Diaz, H. F. 1989: Global climatic anomalies associated with extremes in the Southern Oscillation. *J. Climate*, **2**, 1069–1090.

Klein, S. A., Soden, B. and Lau, N.-C. 1999: Remote sea surface temperature variations during ENSO: evidence for a tropical atmospheric bridge. *J. Climate*, **12**, 917–932.

Krishnamurti, T., Kishtawal, C., LaRow, T., Bachiochi, D., Zhang, Z., Williford, E., Gadgil, S. and Surendran, S. 1999: Improved weather and seasonal climate forecasts from multimodel superensemble. *Science*, **285**, 1548–1550.

Lamb, P. J. 1978: Case studies of tropical Atlantic surface circulation patterns during recent sub-Saharan weather anomalies: 1967 and 1968. *Mon. Wea. Rev.*, **106**, 482–491.

Lamb, P. J. and Peppler, R. A. 1992: Further case studies of tropical Atlantic surface atmospheric and oceanic patterns associated with sub-Saharan drought. *J. Climate*, **5**, 476–488.

Lau, K. M., Shen, S. S. P., Kim, K.-M. and Wang, H. 2006: A multimodel study of the twentieth-century simulations of Sahel drought from the 1970s to 1990s. *J. Geophys. Res.* doi:10.1029/2005JD006281.

Lindzen, R. S. and Nigam, S. 1987: On the role of sea surface temperature gradients in forcing low-level winds and convergence in the Tropics. *J. Atmos. Sci.*, **44**, 2418–2436.

Lohmann, U., Feichter, J., Penner, J. and Leaitch, R. 2000: Indirect effect of sulfate and carbonaceous aerosols: a mechanistic treatment. *J. Geophys. Res.*, **105**, 12193–12206.

Lu, J. and Delworth, T. L. 2005: Oceanic forcing of late 20^{th} century Sahel drought. *Geophys. Res. Lett.*, **32**, L22706. doi:10.1029/2005GL023316.

Lyon, B. 2004: The strength of El Ni˜no and the spatial extent of tropical drought. *Geophys. Res. Lett.*, **31**, L21204. doi:10.1029/2004GL020901.

Mason, S. J. 2001: El Ni˜no, climate change, and southern African climate. *Environmetrics*, **12**, 327–345.

Mason, S. J. and Tyson, P. D. 2000: The occurrence and predictability of droughts over southern Africa. pp. 113–134. in ”Drought - A global assessment”, edited by D. A. Wilhite.

Menon, S., Hansen, J., Nazarenko, L. and Luo, Y. 2002: Climate effects of black carbon aerosols in China and India. *Science*, **297**, 2250–2253.

Mitchell, J. F. B., Karoly, D. J., Hegerl, G. C., Zwiers, F. W., Allen, M. R. and Marengo, J. (2001). *Detection of climate change and attribution of causes*. pp. 525–582.

Mulenga, H. M., Rouault, M. and Reason, C. J. C. 2003: Dry summers over northeastern South Africa and associated circulation anomalies. *Clim. Res.*, **25**, 29–41.

Neelin, J. D., Chou, C. and Su, H. 2003: Tropical drought regions in global warming and El Ni˜no teleconnections. *Geophys. Res. Lett.*, **30(24)**, 2275. doi:10.1029/2003GL0018625.

Nicholson, S. and Kim, J. 1997: The relationship of the El Nino-Southern Oscillation to African rainfall. *Int. J. Climatology*, **17**, 117–135.

Nicholson, S. E. 1981: Rainfall and atmospheric circulation during drought periods and wetter years in West Africa. *Mon. Wea. Rev.*, **109**, 2191–2208.

Nicholson, S. E. 1986: The spatial coherence of African rainfall anomalies: interhemispheric teleconnections. *J. Cli. and Appl. Met.*, **25**, 1365–1381.

Nicholson, S. E. 1993: An overview of African rainfall fluctuations of the last decade. *J. Climate*, **6**, 1463–1466.

Nicholson, S. E. 2000: Land surface processes and Sahel climate. *Rev. Geophys.*, **38**, 117–139.

Nicholson, S., Tucker, C. and Ba, M. 1998: Desertification, drought, and surface vegetation: an example from the West African Sahel. *Bull. Amer. Meteor. Soc.*, **79**, 815–829.

Ogallo, L. J. 1989: The spatial and temporal patterns of the East African seasonal rainfall derived from principal component analysis. *Int. J. Climatology*, **9**, 145–167.

Palmer, T. N. 1986: Influence of the Atlantic, Pacific and Indian Oceans on Sahel rainfall. *Nature*, **322**, 251–253.

Petit-Maire, N. 2002: Sous le sable ... des lacs. Un voyage dans le temps. CNRS Editions, Paris.

Prince, S. D., Brown De Coulston, E. and Kravitz, L. L. 1998: Evidence from rain-use efficiencies does not indicate extensive Sahelian desertification. *Global Change Biology*, **4**, 359–374.

Rasmusson, E. M. and Carpenter, T. H. 1982: Variations in tropical sea surface temperature and surface wind fields associated with the Southern Oscillation/El Ni˜no. *Mon. Wea. Rev.*, **110**, 354–384.

Reason, C. J. C. and Jagadheesha, D. 2005: A model investigation of recent ENSO impacts over southern Africa. *Meteorol. Atmos. Phys.*, **89**, 181–205.

Richard, Y., Trzaska, S., Roucou, P. and Rouault, M. 2000: Modification of the southern African rainfall variability/ENSO relationship since the late 1960s. *Clim. Dyn.*, **16**, 883–895.

Ropelewski, C. F. and Halpert, M. S. 1987: Global and regional precipitation patterns associated with the El Ni˜no/Southern Oscillation. *Mon. Wea. Rev.*, **115**, 1606–1626.

Rotstayn, L. and Lohmann, U. 2002: Tropical rainfall trends and the indirect aerosol effect. *J. Climate*, **15**, 2103–2116.

Rowell, D. P. 2001: Teleconnections between the tropical Pacific and the Sahel. *Q. J. R. Meteorol. Soc.*, **127**, 1683–1706.

Rowell, D. P., Folland, C. K., Maskell, K. and Ward, M. N. 1995: Variability of summer rainfall over tropical North Africa (1906-92): observations and modeling. *Q. J. R. Meteorol. Soc.*, **121**, 669–704.

Santer, B. D., Wigley, T. M. L., Barnett, T. and Anyamba, E. (1996). *Detection of Climate Change and Attribution of Causes*. Cambridge University Press, Cambridge. pp. 407–444.

Schreck, C. J. and Semazzi, F. H. M. 2004: Variability of the recent climate of eastern Africa. *Int. J. Climatol.*, **24**, 681–701.

Seleshi, Y. and Demaree, G. 1995: Rainfall variability in the Ethiopian and Eritrean highlands and its links with the Southern Oscillation Index. *J. Biogeogr.*, **22**, 945–952.

Sobel, A. H., Held, I. M. and Bretherton, C. S. 2002: The ENSO signal in tropical tropospheric temperature. *J. Climate*, **15**, 2702–2706.

Soden, B. J. 2000: The sensitivity of the tropical hydrological cycle to ENSO. *J. Climate*, **13**, 538–549.

Song, Q., Vecchi, G. A. and Rosati, A. J. 2006: Indian Ocean variability in the GFDL coupled climate model. *J. Climate*. in press.

Stott, P. A., Mitchell, J. F. B., Allen, M. R., Delworth, T. L., Gregory, J. M., Meehl, G. A. and Santer, B. D. 2006: Observational Constraints on Past Attributable Warming and Predictions of Future Global Warming. *Journal of Climate*, **19**, 3055–3069.

Taylor, C. M., Lambin, E. F., Stephenne, N., Harding, R. J. and Essery, R. L. H. 2002: The influence of land use change on climate in the Sahel. *J. Climate*, **15**, 3615–3629.

Timmermann, A., Oberhuber, J., Bacher, A., Esch, M., Latif, M. and Roeckner, E. 1999: Increased El Ni˜no frequency in a climate model forced by future greenhouse warming. *Nature*, **398**, 694–697.

Trenberth, K. E. and Hoar, T. J. 1997: El Ni˜no and climate change. *Geophysical Research Letters*, **23**, 3057–3060.

Trenberth, K. E., Dai, A., Rasmussen, R. M. and Parsons, D. B. 2003: The changing character of precipitation. *Bull. Amer. Meteor. Soc.*, **84**, 1205–1217.

Tucker, C. J., Dregne, H. E. and Newcomb, W. W. 1991: Expansion and contraction of the Sahara desert from 1980 to 1990. *Science*, **253**, 299–301.

Unganai, L. 1996: Historic and future climatic change in Zimbabwe. *Clim. Res.*, **6**, 137–145.

von Storch, H. and Zwiers, F. W. 1999: Statistical analysis in climate research. 484 pp. Cambridge University Press.

Vose, R. S., Schmoyer, R. L., Steurer, P. M., Peterson, T. C., Heim, R., Karl, T. R. and Eischeid, J. 1992: The Global Historical Climatology Network: long-term monthly temperature, precipitation, sea level pressure, and station pressure data. ORNL/CDIAC-53, NDP-041. Carbon Dioxide Information Analysis Center, Oak Ridge National Laboratory, Oak Ridge, Tennessee. 300 pp.

Wagner, R. and DaSilva, A. 1994: Surface conditions associated with anomalous rainfall in the Guinea coastal region. *Int. J. Climatology*, **14**, 179–199.

Wallace, J. M., Rasmusson, E. M., Mitchell, T. P., Kousky, V. E., Sarachik, E. S. and von Storch, H. 1998: On the structure and evolution of ENSO-related climate variability in the tropical Pacific: lessons from TOGA. *J. Geophys. Res.*, **103(C7)**, 14241–14259.

Ward, M. N. 1998: Diagnosis and short-lead time prediction of summer rainfall in tropical North Africa at interannual and multidecadal timescales. *J. Climate*, **11**, 3167–3191.

Washington, R., Harrison, M. and Conway, D. 2004: African climate report. UK Department of Environment Food and Rural Affairs, and UK Department for International Development. http://www.defra.gov.uk/environment/climatechange/ccafrica-study/.

Webster, P. 1994: The role of hydrological processes in ocean-atmosphere interaction. *Rev. Geophys.*, **32**, 427–476.

Yulaeva, E. and Wallace, J. M. 1994: The signature of ENSO in global temperature and precipitation fields derived from the microwave sounding unit. *J. Climate*, **7**, 1719–1736.

Figure captions

1. Climatologies of precipitation and near-surface winds for a domain centered on tropical Africa. Precipitation was produced by the Global Precipitation Climatology Project (Huffman et al. 1997) combining satellite estimates and rain-gauge measurements (contours are drawn every 4 mm/day). Winds at the 850hPa pressure level - approximately 3000m above sea level - are from the NCEP-NCAR Reanalysis Project (Kalnay et al. 1996). Panels are for April, July, October and January averages over 1979-2004.

2. Regional averages of annual mean (July-June) precipitation over 1930-2005; the three regions are western (0°N to 20°N, 20°W to 20°E), eastern equatorial (10°S to 10°N, 20°E to 50°E), and southern Africa (25°S to 10°S, 20°E to 40°E). CRU data is depicted in black bars, GPCP in the solid red line. The CRU climatology over 1930-1995 is depicted in the green horizontal line, that of GPCP, over 1979-2005, is depicted in the brown horizontal line.

3. The three leading patterns of a Principal Component Analysis performed on annual mean (July-June) precipitation over Africa during 1930-1995. a, b, c: The spatial patterns, obtained by linear regression of the time series in d,e,f onto precipitation - anomalies are in color, in mm/month, while the contours delimit regions where regression is statistically significant at the 5% level. d, e, f: The associated time series (in units of standard deviation). Note that the upward trend in (d) indicates increasingly stronger values of the negative anomalies in the pattern in (a), i.e. a drying trend. g, h, i: Regression patterns of the time series in d,e,f with sea surface temperature (Kaplan et al. 1998). Anomalies are in contour, spaced every 0.05°C, and dashed in the case of negative values; the presence of color represents their statistical significance at a level of 5% or higher.

4. The difference (XX-PI) between late 20th century (1975-1999) climate in the XX simulations and pre-industrial climate, as estimated from a 25-year mean from the PI simulations. The left panels refer to annual mean surface temperature, the right panels to annual mean precipitation. Warm colors indicate positive and cool colors negative anomalies. The top panels are the mean across all 19 models (the shading interval is 0.1°C for temperature and 0.03mm day^{-1} for precipitation), the solid black line in the right panel is the 4mm day^{-1} contour in the XX simulations and indicates the

location of mean maximum rainfall . The bottom panels are a measure of inter-model agreement: a value of 1 (-1) was assigned at every gridpoint and for every model if the XX-PI difference was positive (negative) and larger than a threshold (0.4° C or 0.05 mm day^{-1}) value; the panels show the sum over all models as percentages (shading interval is every 10%, contour interval is every 20%).

5. As for figure 4, but for the A1B-XX difference. In the top panels, the shading (contour) interval is 0.6°C (0.3°C) for temperature and 0.15 mm day^{-1} (0.2 mm day^{-1}) for rainfall. In the bottom left panel the threshold is 2°C, while in the bottom right panel it is 0.1 mm day^{-1}.

6. Regional averages of precipitation in the IPCC 4AR model simulations; 20th century simulations from 1950 to 2000, and A1B scenario simulations from 2000 to 2100. Regions are defined as in figure 2. Each grey line represents one model, and the thicker black line is the multi-model mean.

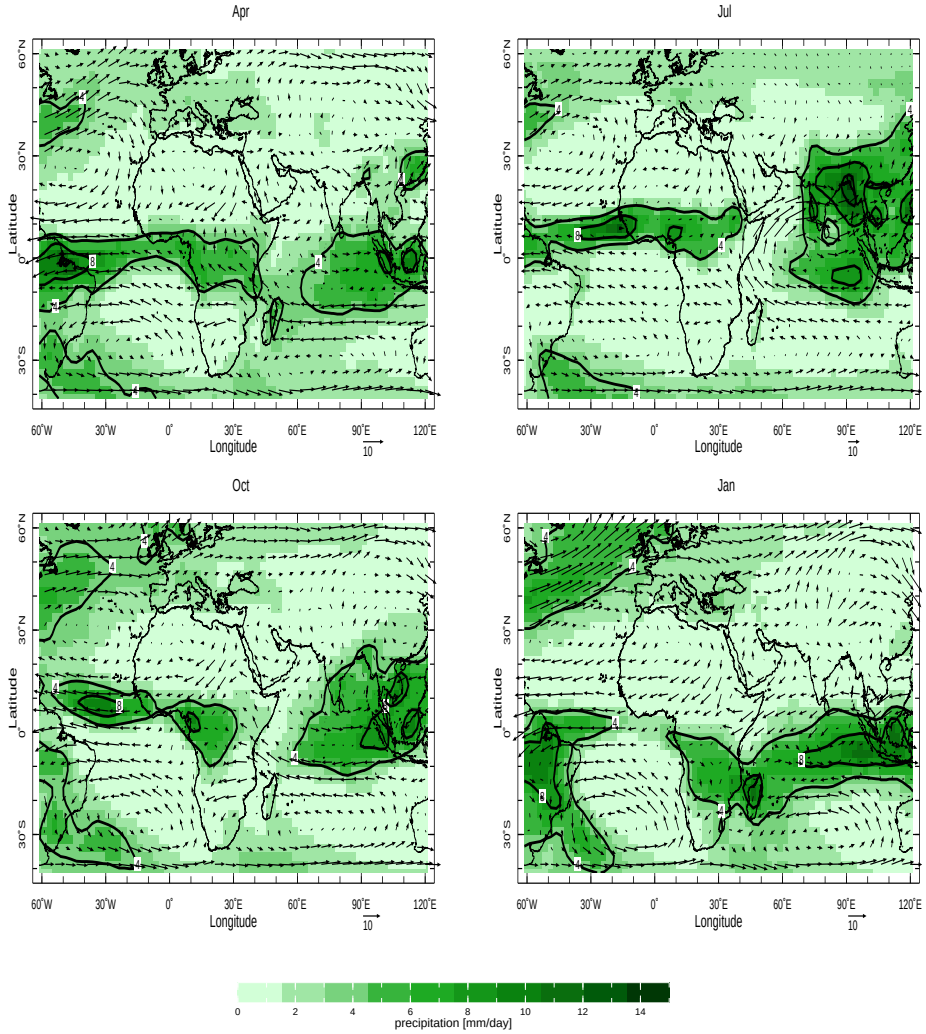

Figure 1. Climatologies of precipitation and near-surface winds for a domain centered on tropical Africa. Precipitation was produced by the Global Precipitation Climatology Project (Huffman et al. 1997) combining satellite estimates and rain-gauge measurements (contours are drawn every 4 mm/day). Winds at the 850hPa pressure level - approximately 3000m above sea level - are from the NCEP-NCAR Reanalysis Project (Kalnay et al. 1996). Panels are for April, July, October and January averages over 1979-2004.

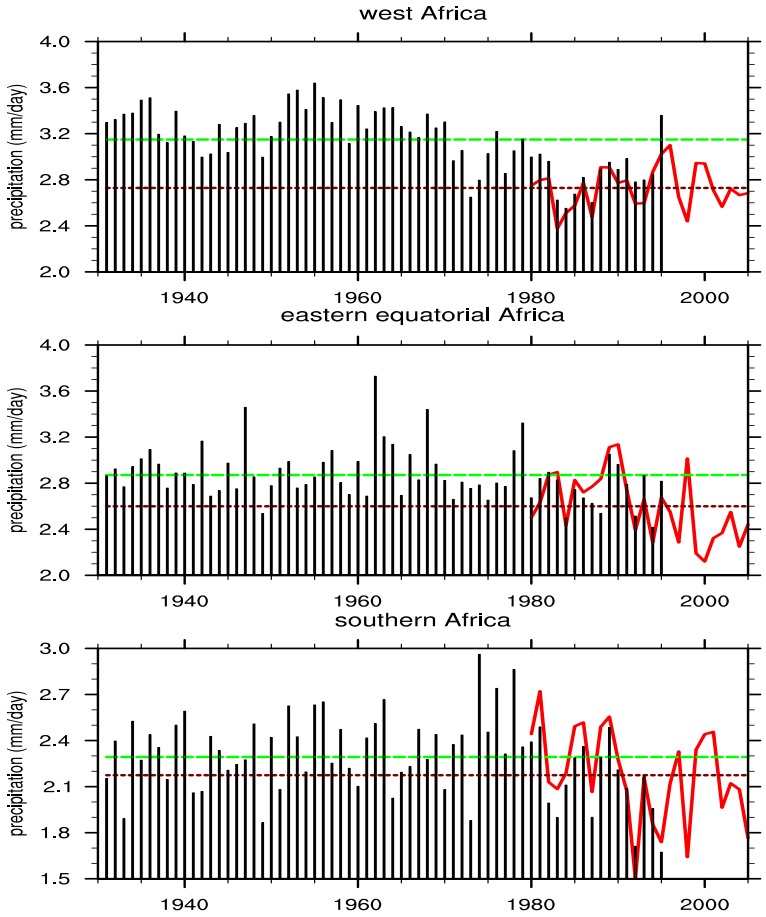

Figure 2. Regional averages of annual mean (July-June) precipitation over 1930-2005; the three regions are western (0°N to 20°N, 20°W to 20°E), eastern equatorial (10°S to 10°N, 20°E to 50°E), and southern Africa (25°S to 10°S, 20°E to 40°E). CRU data is depicted in black bars, GPCP in the solid red line. The CRU climatology over 1930-1995 is depicted in the green horizontal line, that of GPCP, over 1979-2005, is depicted in the brown horizontal line.

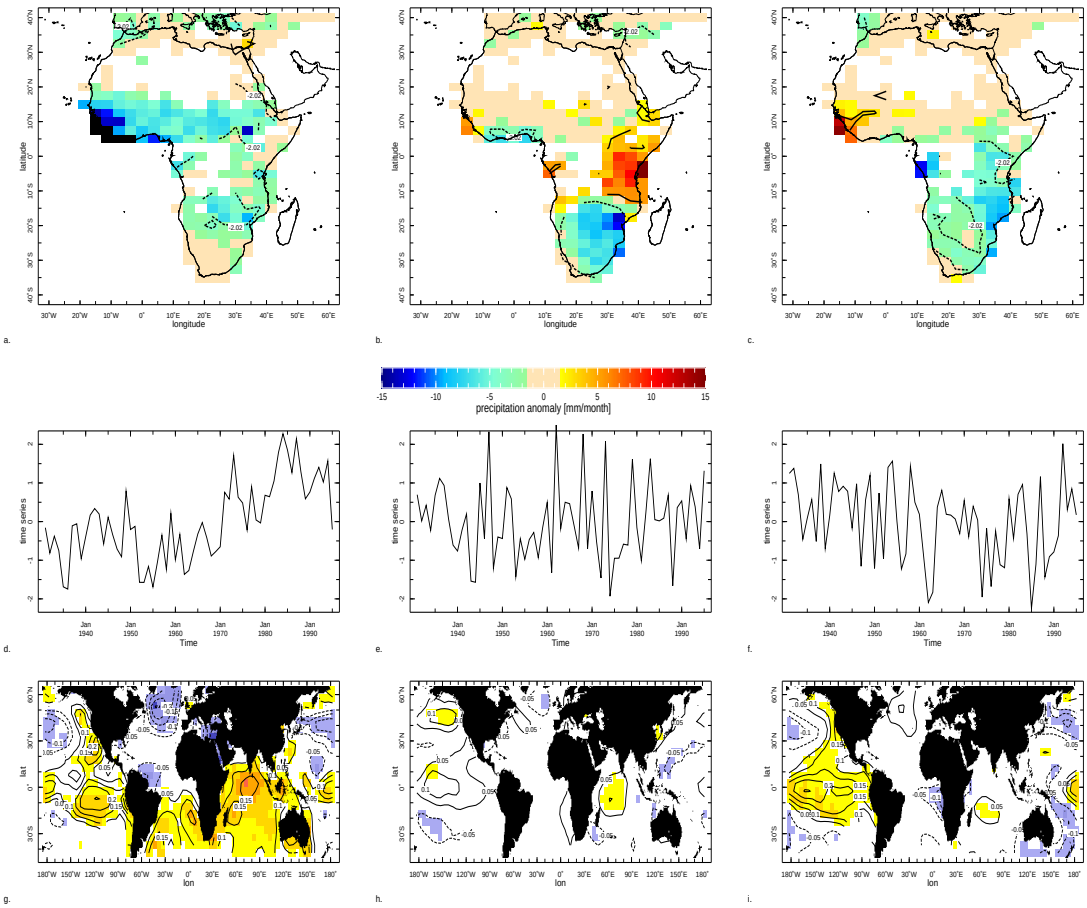

Figure 3. The three leading patterns of a Principal Component Analysis performed on annual mean (July-June) precipitation over Africa during 1930-1995. a, b, c: The spatial patterns, obtained by linear regression of the time series in d,e,f onto precipitation - anomalies are in color, in mm/month, while the contours delimit regions where regression is statistically significant at the 5% level. d, e, f: The associated time series (in units of standard deviation). Note that the upward trend in (d) indicates increasingly stronger values of the negative anomalies in the pattern in (a), i.e. a drying trend. g, h, i: Regression patterns of the time series in d,e,f with sea surface temperature (Kaplan et al. 1998). Anomalies are in contour, spaced every 0.05°C, and dashed in the case of negative values; the presence of color represents their statistical significance at a level of 5% or higher.

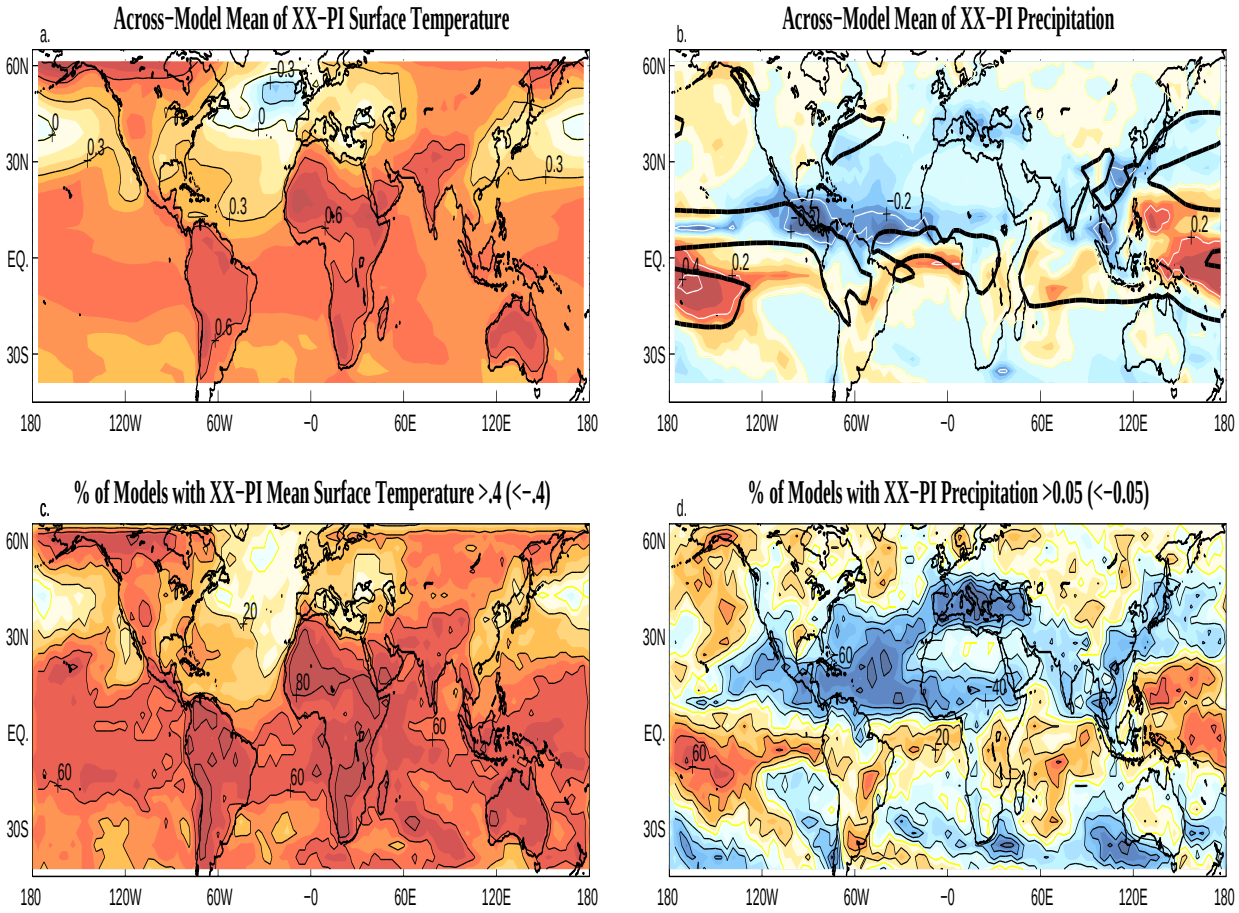

Figure 4. difference (XX-PI) between late 20th century (1975-1999) climate in the XX simulations and pre-industrial climate, as estimated from a 25-year mean from the PI simulations. The left panels refer to annual mean surface temperature, the right panels to annual mean precipitation. Warm colors indicate positive and cool colors negative anomalies. The top panels are the mean across all 19 models (the shading interval is 0.1°C for temperature and 0.03mm day^{-1} for precipitation), the solid black line in the right panel is the 4mm day^{-1} contour in the XX simulations and indicates the location of mean maximum rainfall . The bottom panels are a measure of inter-model agreement: a value of 1 (-1) was assigned at every gridpoint and for every model if the XX-PI difference was positive (negative) and larger than a threshold (0.4° C or 0.05 mm day^{-1}) value; the panels show the sum over all models as percentages (shading interval is every 10%, contour interval is every 20%).

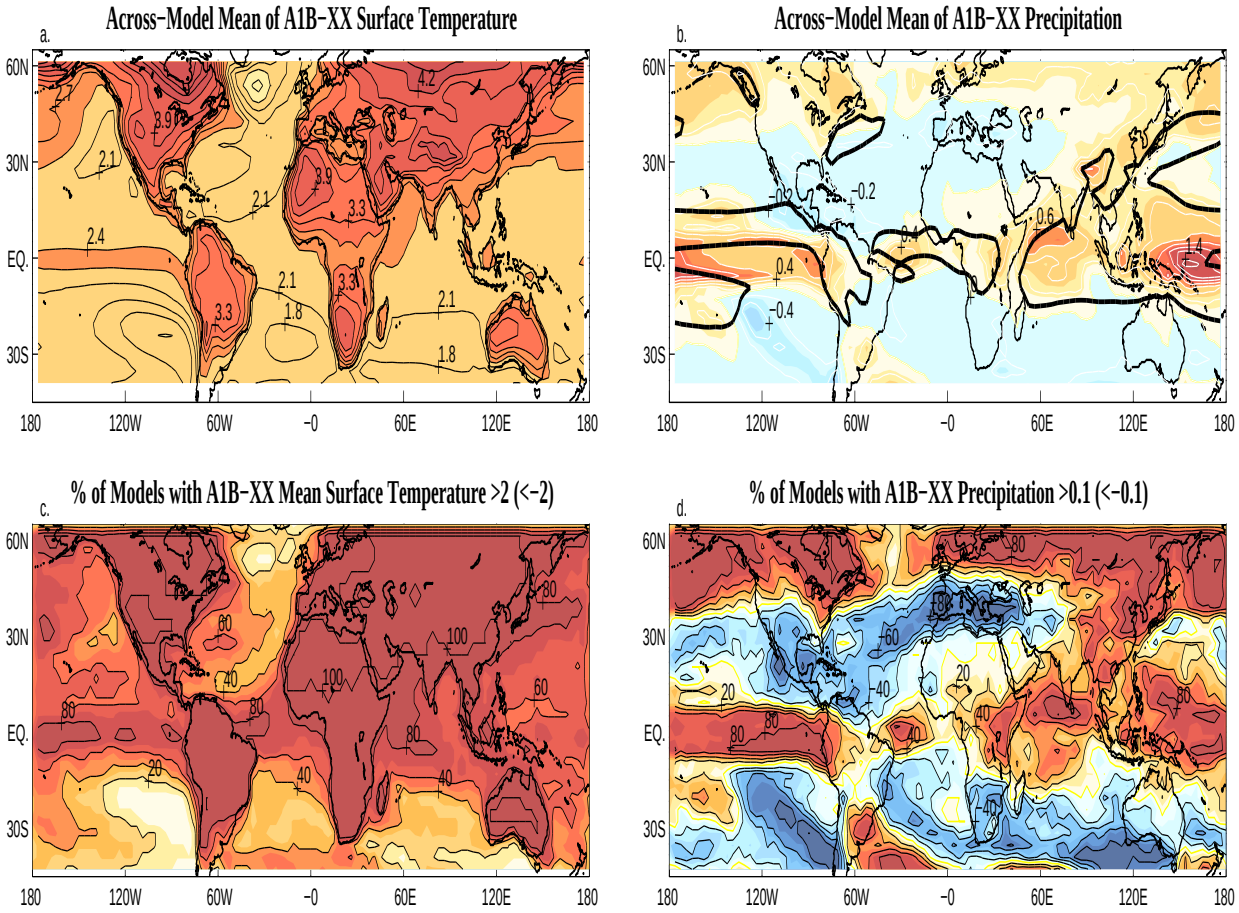

Figure 5. As for figure 4, but for the A1B-XX difference. In the top panels, the shading (contour) interval is 0.6°C (0.3°C) for temperature and 0.15 mm day^{-1} (0.2 mm day^{-1}) for rainfall. In the bottom left panel the threshold is 2°C, while in the bottom right panel it is 0.1 mm day^{-1}.

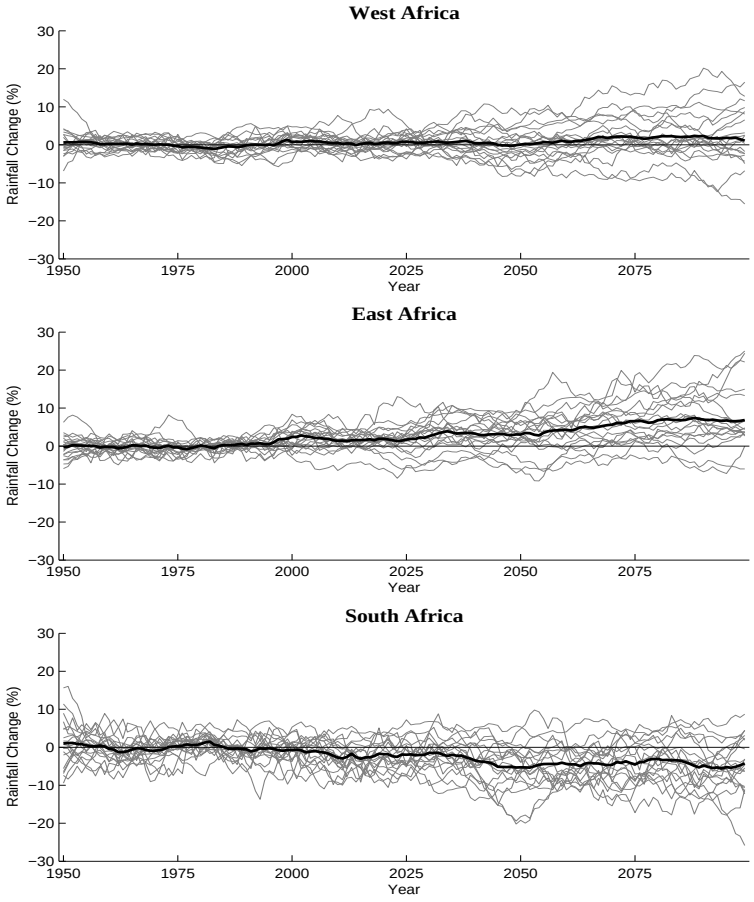

Figure 6. Regional averages of precipitation in the IPCC 4AR model simulations; 20th century simulations from 1950 to 2000, and A1B scenario simulations from 2000 to 2100. Regions are defined as in figure 2. Each grey line represents one model, and the thicker black line is the multi-model mean.